2ème Conférence Internationale des Energies Renouvelables CIER-2014
Proceedings of Engineering and Technology - PET

Design and Tuning of Different PID Controllers for Variable Speed Induction Motor

Salima Lekhchine[#1], Tahar Bahi[#2], Issam Abadlia[*3], Hamza Bouzeria[*4], Zakaria Layate[#5]

[#1]*Department of Electrical Engineering, 20 August 1955-Skikda University,Skikda 21000, Algeria*
[#1]slekhchine@yahoo.fr
[2,3,5]*Department of Electrical Engineering, Badji Mokhtar University,BP 12, Annaba 23000, Algeria*
[#2]tbahi@hotmail.com; [*3]i_abadlia@yahoo.fr; [#5]zakarialayate@gmail.com
[*4]*Department of Electrical Engineering, Hadj Lakhdar University, Batna 05000, Algeria*
[*4]bhamza23000@gmail.com

***Abstract*— Proportional Integral Derivative (PID) controllers comprise about 95% of controllers used in industry. The design and tuning of these controllers are still a major area of research. In this paper four PIDs shams for variable-speed induction motor using indirect field oriented control strategy are used, with further discussion, these controllers are: PI with a pre-filter, IP, anti-windup IP and variable-gains anti-windup IP. Conventional methods are used for tuning gains of the three first's controllers. The last method is needed to develop an adaptative control based on variable-gains anti-windup IP controller. The obtained simulation result by Matlab/Simulink showed the performances of each controller and demonstrates the altitudes of the last technique on speed control regulation when compared to the others methods design.**

***Keywords*— Induction Motor; Indirect Field Oriented Control; PID Controller; Anti-windup; Variable-gains.**

NOMENCLATURE

s, r : stator and rotor indices
d,q : frame axes indices
R_s, R_r : stator and rotor resistances
L_s, L_r , $_{Lm}$: stator, rotor and magnetizing inductances
J: motor inertia
f: viscous coefficient
p: number of pairs poles
φ_s , φ_r : stator and rotor flux
i_s, i_r: stator and rotor courent
T_l : load torque
T_e : electromagnetic torque
ω_s : stator pulsation
ω_r : rotor pulsation
s, ω_{sl} : slip and slip frequency
Ω_r : rotor speed (rd/s)
σ : leake flux total coefficient
θ_s : Park transformation angle

I. INTRODUCTION

It is well-known that the induction motor (IM) has the advantages of simplicity, efficiency and low cost when compared to the DC motor and synchronous motor [1]. So, an IM is often used for the commercial Alternative Current (AC) drive. Then, the research and manufacture of AC drives become more popular and competitive. However, IM has disadvantages, such as complex, nonlinear, and multivariable of mathematical model, what's more the induction motor is not inherently capable of providing variable speed operation [2]. Conventional control of an IM is difficult due to strong nonlinear magnetic saturation effects and temperature dependency of the motor's electrical parameters. As the conventional control approaches require a complex mathematical model of the induction motor to develop PID controllers for quantities such as speed, torque, and position.

Most of the research on the drive design of the IM concentrated on the modern control design, such as Sliding Mode Control [3], Fuzzy Logic Control [4], Neural Networks Control [5], H_∞ Control [6], Neural-Fuzzy Control [7], etc. If the prices of memory and Digital Signal Processor (DSP) chip are much cheaper than now, those control algorithms will be adopted in various applications. However, in order to be compatible with the conventional drives, a PID control is generally considered in IM drive.

In the paper an extension design of different PID controllers for variable-speed IM using indirect field oriented control strategy is used to tune gains in speed closed-loop control system for IM drives. The main contributions of this paper are:

1) Presentations and brief overviews of design and tuning diverse PID controllers for variable-speed induction motor. There devises controllers are: PI with a pre-filter, IP, anti-windup IP and variable gains anti-windup IP.

2) In order to improve the behavior of the speed control, based on [8], an adaptative variable gains anti-windup IP speed controller is developed.

3) A performing comparative study between the proposed speed controllers design demonstrate the performances of each regulator.

The paper is divided into five branches with more discussion as follows: section I, introduction; section II, induction motor and its drive; section III, the proposed speed controllers design; section IV, simulation results; section V, conclusion and a reference list at the last.

II. System Description And Control

Under some usual assumptions, the IM dynamic model in the rotating field reference frame can be presented by the following [9]:

$$\begin{cases} \frac{d}{dt} i_{ds} = \frac{1}{\sigma L_s}\left[-R_{sr} i_{ds} + \omega_s \sigma L_s i_{qs} + \frac{L_m R_r}{L_r^2}\varphi_{dr} + \frac{L_m}{L_r}\omega\varphi_{dr} + V_{ds} \right] \\ \frac{d}{dt} i_{qs} = \frac{1}{\sigma L_s}\left[-R_{sr} i_{qs} - \omega_s \sigma L_s i_{ds} + \frac{L_m R_r}{L_r^2}\varphi_{qr} + \frac{L_m}{L_r}\omega\varphi_{qr} + V_{qs} \right] \\ \frac{d}{dt}\varphi_{dr} = \frac{L_m R_r}{L_r} i_{ds} - \frac{R_r}{L_r}\varphi_{dr} + \omega_{sl}\varphi_{qr} \\ \frac{d}{dt}\varphi_{qr} = \frac{L_m R_r}{L_r} i_{qs} - \frac{R_r}{L_r}\varphi_{qr} - \omega_{sl}\varphi_{dr} \end{cases} \quad (1)$$

Where $R_{sr} = \left(R_s + R_r \frac{L_m^2}{L_r} \right)$, $\sigma = \left(1 - \frac{L_m^2}{L_s L_r} \right)$

and $\omega_{sl} = \omega_s + p\omega_r$, $\sigma = \left[1 - \left(L_m^2 / L_s L_r \right) \right]$

The electromagnetic torque is given by:

$$T_e = p \frac{L_m}{L_r} \left(\varphi_{dr} i_{qs} + \varphi_{qr} i_{ds} \right) \quad (2)$$

According to FOC theory, by requiring $\varphi_{dr}^* = \varphi_r^*$ and $\varphi_{qr}^* = 0$, the IM equations in the synchronous reference become.

$$\begin{cases} V_{ds} = \left(R_s + s\sigma L_s \right) i_{ds} - \omega_s \sigma L_s i_{qs} \\ V_{qs} = \left(R_s + s\sigma L_s \right) i_{qs} + \omega_s \sigma L_s i_{ds} + \omega_s \frac{L_m}{L_r}\varphi_r \end{cases} \quad (3)$$

With, $\omega_{sl}^* = \frac{L_m}{T_r \varphi_{dr}^*} i_{qs}$ (4)

And, $\omega_s^* = \omega_{sl}^* + p\omega_r$ (5)

The electromagnetic torque expression is thereby reduced to:

$$T_e^* = p \frac{L_m}{L_r} \varphi_{dr}^* i_{qs}^* \quad (6)$$

These equations show that the flux will depend only on ids, and if this latter is maintained constant, the torque will depend only on i_{qs}. However, in the case of a power voltage supply, as shown in system (3), V_{ds} and V_{qs} influence both i_{ds} and i_{qs}; and consequently affect the flux and the torque. To avoid this dependency, it is common to add compensation terms after the ids and i_{qs} controllers. These terms are given as follows:

$$\begin{cases} \bar{V}_{ds} = -\omega_s \sigma L_s i_{qs} \\ \bar{V}_{qs} = \omega_s \sigma L_s i_{ds} + \omega_s \frac{L_m}{L_r}\varphi_r^* \end{cases} \quad (7)$$

A scheme of an induction motor based on indirect field oriented control (IFOC) strategy is illustrated by Fig. 1. It mainly consists of an outer speed loop and inner loops for currents. Never-the less, the draw back of this control strategy is its inner loops dependency on both stator resistance and rotor time constant changes ((3), (4)). The stator resistance mismatch is generally neglected given that the inner loops are usually synthesized so that they enforce a static gain equal to one and a very small response time when compared to the speed one. While the rotor time constant change, which deteriorate the IFOC decoupling and performances by affecting ω_{sl} (4) and thereby θ_s, could be avoided only by accurate real time estimation. However, the above drawback can not affect our conclusions about the compared speed controllers, since their corresponding induction motor speed drives employ the same IFOC scheme.

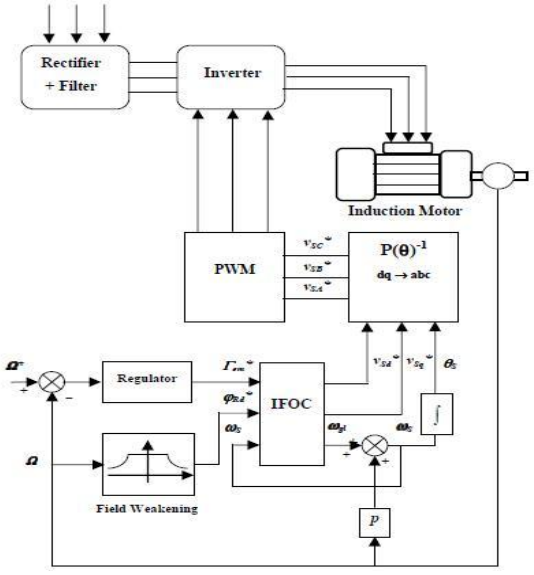

Fig. 1 Bloc diagram of indirect field oriented control

III. SPEED CONTROLLERS DESIGN

In this section, the structures of the PIDs speed controllers for variable-speed induction motor are introduced. These controllers are: PI with a pre-filter, IP, anti-windup IP and variable gains anti-windup IP.

A) PI controller with a pre-filter

The classic numerical PI (Proportional and Integral) regulator is well suited to regulating the speed (Ω), to the desired values (Ω^*) as it is able to reach constant reference, by correctly both the P term (K_p) and I term (K_i) winches are respectively responsible for error (e) sensibility and for the steady state error. The dynamic model of speed induction motor drive with PI is significantly simplified, and can be reasonably represented by the bloc diagram shown in Fig. 2.

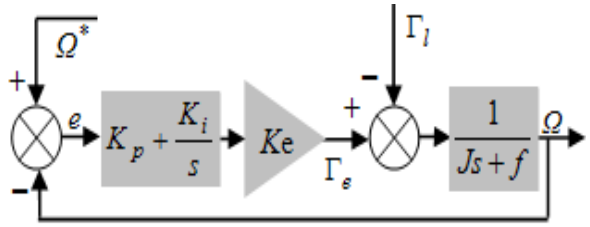

Fig. 2 IM speed control loop with PI controller

with $K_e = p.\frac{L_m}{L_r}.\varphi_r^*$ is the torque constant.

If $T_l = 0$, the open loop transfer function with PI controller is as following (6)

$$G(s) = \frac{\Omega}{\Omega^*} = \frac{K_e\left(K_p s + K_i\right)}{Js^2 + fs} \tag{8}$$

The speed PI together with the mechanical plant will be reduced to a pure second order system as shown in (9)

$$T(s) = \frac{\omega_n^2}{s^2 + 2\xi\omega_n.s + \omega_n^2} \tag{9}$$

If $\varphi_r^* = \varphi_n$, the closed loop transfer function from the mechanical loop with the tuned PI gives not only the desired pure second order system, but also an unwanted zero, which worsens the transient response.

$$T(s) = \frac{G(s)}{1+G(s)} = \frac{\frac{K_i}{J}\left(\frac{K_p}{K_i}s+1\right)}{s^2 + s\left(\frac{f}{J}+\frac{K_p}{J}\right)+\frac{K_i}{J}} \tag{10}$$

The solution to have a pure second order system is to insert a pre-filter (F(s)) to get rid of the unwanted zero (11)

$$F(s) = \frac{1}{\tau_F s + 1} \tag{11}$$

with: $\tau_F = \frac{K_p}{K_i}$ is the filter constant time.

Fig. 3 shows the speed closed loop with PI and a pre-filter, also the system's behavior is equal to the desired second order like in (9).

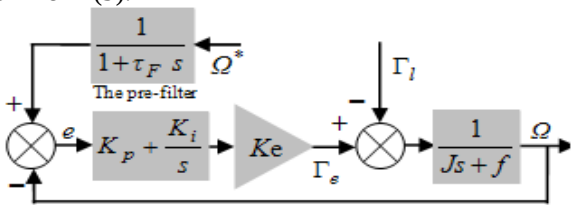

Fig. 3 IM speed control loop with PI and a pre-filter

B) IP controller

The PI controller has a proportional as well as an integral term in the forward path; while the IP controller moves the proportional term to the feedback path and it acts like feedback compensation. To describe the difference between PI and IP controller, schematic the IP controller is depicted in Fig. 4.

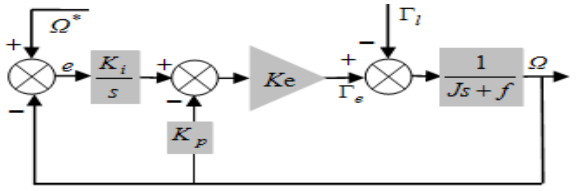

Fig. 4 IM speed control loop with IP controller

Compared with the PI, the IP has the advantages of a smaller overshoot and faster settling time for both step response and load-variation response [10]. This controller type (IP) is derived from the classical Proportional-Integral (PI) controller, but has the advantage of leading to a transfer function in closed loop without zero. The closed loop transfer function with the IP controller is as following (12)

$$H(s) = \frac{1}{\frac{J}{K_p K_i}s^2 + \frac{K_p + f}{K_p K_i}s + 1} \tag{12}$$

To control the closed loop system, it is necessary to choose the K_p, K_i coefficients. In our study the tax pole method [11] is to choose. The transfer function closed loop is characterized by

$$T(s) = \frac{1}{s^2 + 2\xi\omega_n.s + \omega_n^2} \tag{13}$$

By analogy between the expressions (12) and (13) include:

$$\begin{cases} \frac{J}{K_p K_i} = \frac{1}{\omega_n^2} \\ \frac{K_p + f}{K_p K_i} = \frac{2\xi}{\omega_n} \end{cases} \Rightarrow \begin{cases} K_p = 2J\xi\omega_n - f \\ K_i = \frac{J\omega_n^2}{K_p} \end{cases} \tag{14}$$

Corrector gains are obtained for a minimum response time while ensuring not exceeded. This technique relates to impose values ξ and ω_n for determining the coefficients K_p and K_i.

C) Anti-windup IP controller

Every real system presents some physic limitations or has some control constraints to safeguard system's integrity. The ideal control, which has been introduced above, is completely valid, although it fails when the input reference or load are deeply changed. Under these conditions, because of the Windup phenomena, the system's performance worsens and eventually it may become unstable [12]. For rings the windup problem, in [8], an anti-windup IP speed controller with a study of a stability conditions is proposed by H. Tsung-Lieh and H. Chao-Ming. The scheme of this controller is illustrated by Fig. 5.

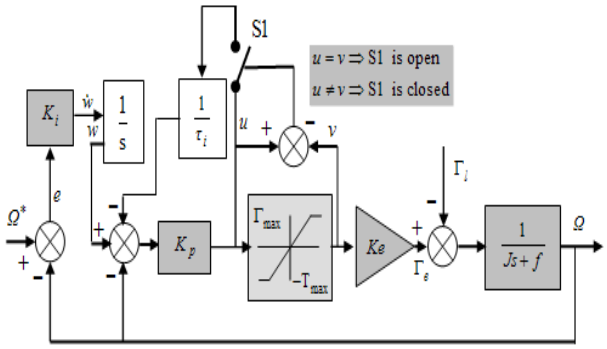

Fig. 5 Schematic diagram of anti-windup IP controller

The main goal of anti-windup scheme is to avoid the over value in the Integrator, therefore the integration output will be kept within a limited range.

The closed loop transfer function IM with anti-windup IP is characterized by:

$$G(s)=\frac{K_p\left(\frac{1}{\tau_i}s+\frac{1}{\tau_i\tau_m}\right)}{s^2\left(\frac{K_pK_e}{J}+\frac{1}{\tau_m}\right)s+\frac{K_pK_e}{\tau_iJ}} \tag{15}$$

Let $\tau_i = K_p/K_i$ with τ_i is the integral state.

$\tau_m = f/J$: is the mechanical time constant.

As depicted in Fig. 5, the plant input v is limited nonlinearity as follows:

$$v=\begin{cases} u_{\max} & ,if \quad u > u_{\max} \\ u & ,if \quad u_{\min} \le u \le u_{\max} \\ u_{\min} & ,if \quad u < u_{\min} \end{cases} \tag{16}$$

Where $u_{\min}$ and u_{maw} denote the lower and upper bound of u, respectively. The output of the IP anti-windup controller u can be expressed as:

$$u = w - K_p\Omega \tag{17}$$

Where w is the integral state. When the speed command or the external load has a large step change, the output of the anti-windup IP controller u may be saturated. This induces that the plant input is clamped at a prescribed maximum value and the integral state may rapidly converge to zero. Otherwise, the integral state will accumulate the speed error and the IP action is activated. The integral state w can be expressed as follows

$$\dot{w}=\begin{cases} K_ie & ,if \ u=v \\ K_ie-\frac{1}{\tau_i}u & ,if \ u\neq v \end{cases} \tag{18}$$

From (18), it implies that the IP controller is saturated if $u \neq v$, and linear if $u = v$. Equation (18) also assumes that mechanical time constant τ_m is much slower than integral time τ_i .

As shown in (16), the speed controller is operated in either the saturated region or in the linear region. When operating in the saturated region, the anti-windup control strategy will assure that the IP controller can converge toward the linear region. Hence, it is desired to characterize both the domain of attraction when the IP controller is saturated and the asymptotic stability in the linear region.

In [8], tow stability conditions are used:

1) Attractivity condition:

$$|\Gamma_l| < \left(\frac{f}{K_p}-K_e\right)u_{\max} \tag{19}$$

2) Asymptotic stability condition:

$$\left(\frac{1}{\tau_m}+\frac{K_eK_p}{J}\right)|\Omega^*|+\left|\frac{\Gamma_l}{J}\right| \le \frac{K_e}{J}u_{\max} \tag{20}$$

By design an identification methods, stability conditions can be expressed as ((21) and (22))

$$\tau_i \ge \frac{K_pJ}{\sqrt{(K_pK_e+f)^2+K_e{}^2}-K_e} \tag{21}$$

$$|G(j\omega)|^2 \le 1 \tag{22}$$

D) A variable gains anti-windup IP controller

A variable-gain anti-windup IP speed controller is developed in order to minimize some degree of the variations parameters effects of the induction motor. Variable-gains $(K_p,\ K_i)$ is an adaptative algorithm for anti-windup IP controller is realized for to conditions stands on stability study of an anti-windup IP.

Based on (19), (21) and (22), K_p and K_i gains are limited as follows ((23) and (24)):

$$\begin{cases} K_p \le \frac{f\Gamma_l}{K_e\Gamma_l-u_{\max}} & ,if\ \Gamma_l \le 0 \\ K_p > \frac{f\Gamma_l}{K_e\Gamma_l+u_{\max}} & ,if\ \Gamma_l > 0 \end{cases} \tag{23}$$

$$K_i \ \max \ge \frac{\sqrt{(1/2)*(K_pK_e+f)^2+K_e{}^2}-K_e}{K_pJ} \ge K_i \ \min \tag{24}$$

IV. Simulation Results

Based on (23) and (24), the limits values gains of the variable-gains anti-windup IP controller are

$$\begin{cases} K_p = [K_p\,\min \quad K_p\,\max] = [2.6133 \quad 7.6848] \\ K_i = [K_i\,\min \quad K_i\,\max] = [26.3212 \quad 38.4982] \end{cases}$$

Fig. 6 shows the Nyquist Diagram of closed loop G(s) transfer function with conditions stability. Were $(K_i\,\min)$ and $(K_i\,\max)$ reporters the stability conditions designates respectively (21) and (22) also defined stability zone function of the variable-gains anti-windup IP speed controller.

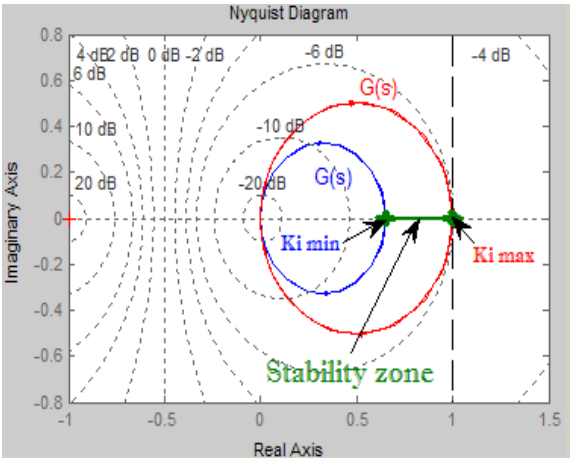

Fig. 6 Nyquist Diagram of G(s)

Fig. 7 shows the response of speed for different controllers design.

1. *Step-Response*

By a zoom of speed response, Fig. 7, figures 8 and 9 shows the response of speed for different controllers at $100\,\text{rad/s}$ and $-100\,\text{rad/s}$ respectively. The Table 2 illustrates the performances criteria of each controller at $100\,\text{rad/s}$, including rise time, overshoot and settling time. Simulation results obtained from windup and non-windup cases reveal that the proposed variable-gains anti-windup IP control method can provide superior performances such as very small overshoot, faster settling time, and a best rise time better the other control methods.

2. *Load-Variation*

To verify the dynamic performance of the proposed methods, load-variation was also executed. Fig. 10 depicts the speed with the load increased $(\Gamma_l = 20\,\text{N.m})$ for different controllers at $100\,\text{rad/s}$. The load was increased a $t = 0.25\text{s}$. The simulation results reveal that the proposed variable-gains anti-windup IP controller has the superior performances of load disturbance than the other methods.

3. *Rotor resistance -Variation*

Fig. 11 shows the effect of rotor resistance (R_r) on the speed response. In the actual operating conditions, the rate of change of temperature is very slow and so the resistance variation, this is covered in Fig. 11. Where at $t = 0.9\text{s}$ a change of R_r value to 150% R_r is applied. We notice that the adaptative controller present a more best performing when compared to other controllers design.

TABLE 2
PERFORMANCE COMPARISON OF EACH CONTROLLER AT 100 RAD/S

Controller	Performance parameters		
	Rise time	Overshoot	Settling time
PI	0.065	5.3%	0.22
IP	0.17	0%	0.19
Anti-windup IP	0.15	0%	0.17
Variable-gains anti-windup IP	0.055	0.76%	0.068

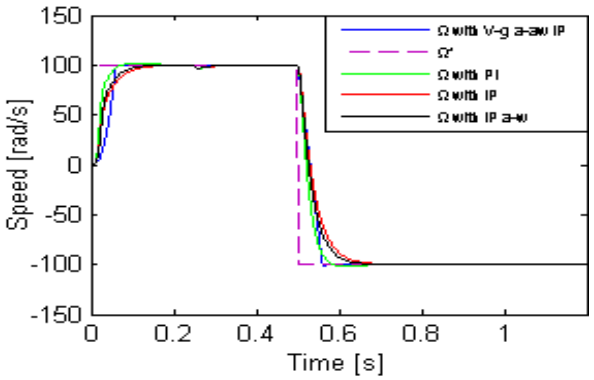

Fig. 7 Speed response for different controllers

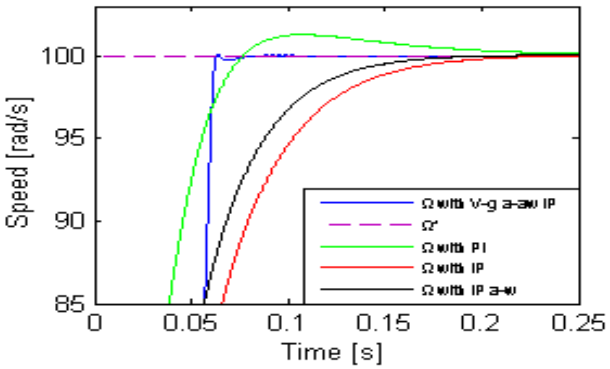

Fig. 8 Zoom of the speed response at $100\,\text{rad/s}$

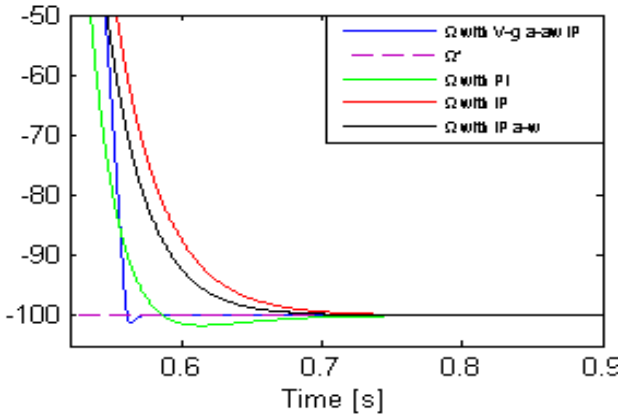

Fig. 9 Zoom of the speed response at $-100\,\mathrm{rad/s}$

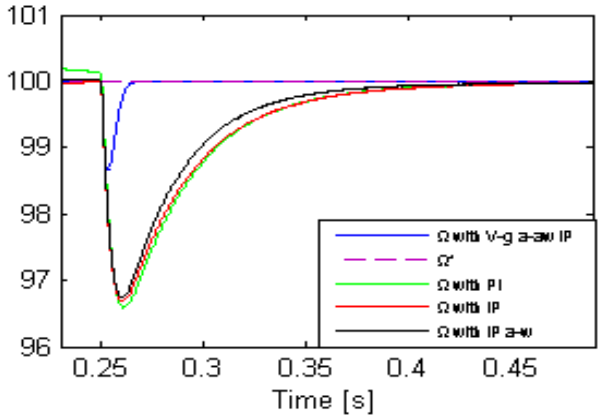

Fig. 10 The speed response with load variation at $t = 0.25\mathrm{s}$

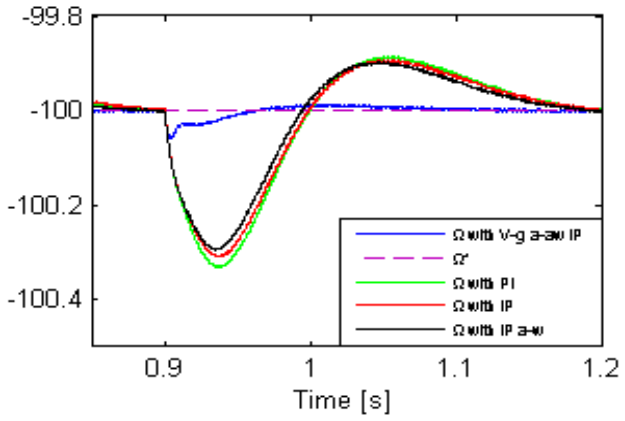

Fig. 11 Speed response with Rotor resistance variation at $t = 0.9\mathrm{s}$

V. Conclusion

The aim of this work has been to address the design, tuning and simulation of different PID speed controllers of an induction motor using indirect field oriented control strategy. These design techniques are based on classical methods. The obtained simulation results indicate more robustness against induction motor parameter variations as well as high disturbance rejection capability of the proposed adaptive structure speed controller compared to fixed structure techniques. The relevant simulation results have been given by MatLab/Simulink.

References

[1] M. Bayindir, H. Can, Z. H. Akpolat, M. Özdemir, & E. Akin, "Application of reaching law approach to the position control of a vector controlled induction motor drive." Electrical Engineering, 87, 207–215, 2005.

[2] P. Pillay and R. Krishnan, "Modeling, Simulation and analysis of Permanent-Magnet Motor Drives, Part II: The Permanent-Magnet Synchronous Motor Drive," IEEE Trans. on Ind. Appl. , vol. 25 , No. 2 , pp.274-279 , 1989.

[3] J. P. Karunadasa, and A. C. Renfrew, "Design and Implementation of Microprocessor Based on Sliding Mode Controller for Brushless Servomotor," IEE Proceedings B Electric Power Applications, Vol. 138, No. 6, pp. 345-363, 1991.

[4] B. Kumar, M, Yogesh, K. Chauhan, and V. Shrivastava, " Efficacy of Different Rule Based Fuzzy Logic Controllers for Induction Motor Drive," International Journal of Machine Learning and Computing, Vol. 2, No. 2, April 2012.

[5] M. Zerikat and S. Chekroun, "Adaptation Learning Speed Control for a High-Performance Induction Motor using Neural Networks, "World Academy of Science, Engineering and Technology 21, Vol, 14, No. 7, pp. 293-298, 2008.

[6] J. L. Hsien, Y. Y. Sun, and M. C. Tsai, "H_∞ Control for a Sensorless permanent-magnet Synchronous Drive," IEE Proceedings Electric Power Applications, Vol, 144, No. 3, pp.173-181, 1997.

[7] F. J. Lin and C. H. Lin, "A Permanent-magnet Synchronous Motor Servo Drive Using Self-constructing Fuzzy Neural Network Controller," IEEE Transactions on Energy Conversion, Vol. 19, No. 1, pp. 66-72, 2004.

[8] H. Tsung-Lieh and H. Chao-Ming, "Implementation of switched reluctance motor drive system using digital FPGA scheme. " International journal of electrical engineering, Vol.17, no.3 pp.189-197, 2010.

[9] Z. Yan, C. Jin, V.I. Utkin, Sensorless sliding-mode control of induction motors, IEEE Trans. Ind. Electron. 47, 1286–1297, 2000.

[10] C. M. Liaw, & F. J. Lin, "A robust induction motor serve drives." In IEEE international symposium on industrial electronics ISIE'93 pp. 736–740, 1993.

[11] F. J. Lin, R. J. Wai & H. P. Chen, "A PM synchronous servo motor drive with an on-line trained fuzzy neural network controller. " IEEE Transactions on Energy Conversion, 13(4), pp 319–325, 2012.

[12] W. Ming-Shyan, "Design and performance evaluation of industrial brushless servomotor drives. " International Journal of Technology, Vol. 21, No. 3, pp.291-298, 2006.